

## Charge-density analysis of GaS

A. Kuhn and A. Bourdon

*Laboratoire de Luminescence,\* Université Pierre et Marie Curie, 4 place Jussieu, 75230 Paris Cedex 05, France*

J. Rigoult and A. Rimsky

*Laboratoire de Minéralogie-Cristallographie,† Université Pierre et Marie Curie, 4 place Jussieu, 75230 Paris Cedex 05, France*

(Received 21 July 1980)

The electron density in the  $A^{III}B^{VI}$  crystal GaS was experimentally determined by x-ray diffraction. The resulting density distribution varies markedly from the distribution predicted by the pseudopotential model proposed by Schlüter *et al.* The real bonds observed in the x-ray diffraction determined distribution are curved and are located not only between Ga-Ga and Ga-S nearest neighbors as predicted by the pseudopotential model, but also between Ga and S next-nearest neighbors in the same elementary cell, between Ga and S atoms in adjoining elementary cells, and between S-S interlayer neighbors in the same elementary cell. The two atoms Ga and S are highly polarized. These findings allow a better understanding of the bondings and the discrepancies between our experimental findings, and the present pseudopotential model should permit an improvement in a future theoretical model for bonding in the  $A^{III}B^{VI}$  crystals.

## INTRODUCTION

The  $A^{III}B^{VI}$  crystals are characterized by a highly anisotropic layer structure. The layers are made up of four two-dimensional sheets of similar atoms in the sequence chalcogenide-metal-metal-chalcogenide. Within the layers the bonding between chalcogenide and metal atoms is strongly covalent although polarized, while the weak interlayer interactions are of the van der Waals type.<sup>1</sup> Different stacking sequences of the layers are possible in most of these crystals, resulting in different polytypes with different crystalline structures,<sup>2</sup> which exhibit minor variations in their optical<sup>3</sup> and electrical properties.<sup>4</sup>

The optical, semiconducting, photoconducting, and luminescent properties of the  $A^{III}B^{VI}$  crystals have been extensively studied. The band structure was initially calculated by Bassani *et al.*<sup>5-7</sup> (among others) using a semiempirical tight-binding method with a two-dimensional single-layer approximation. Further studies,<sup>8-15</sup> showed that, in spite of the high structural anisotropy, three-dimensional calculations were necessary to account for the experimental findings. Consequently, Schlüter *et al.*<sup>10</sup> proposed a theoretical model derived from calculations using the empirical pseudopotential method based on local spherically sym-

metric potentials. The pseudopotential method uses the pseudo-wave-functions obtained from band calculations to determine charge densities.<sup>10-13</sup> The results of synchrotron-radiation photoemission studies<sup>16</sup> and of x-ray-induced photoemission studies<sup>17</sup> have provided a good fit<sup>13,18</sup> to the pseudopotential model, but only within certain narrow energy regions.

We set out to compare the electronic structure predicted by the pseudopotential method with the experimental determination of electron densities by x-ray diffraction, which provides results for the valence electrons in the entire real space. Initial results using MoK $\alpha$  radiation showed important differences between theoretical predictions and experimental findings. In this paper we present the results of a systematic study of the electron density distribution of the GaS crystal. Our choice of GaS was conditioned by the fact that among  $A^{III}B^{VI}$  crystals, it presents the structure with the highest symmetry, having only one type of structure without stacking faults, the  $\beta$  type with the symmetry  $P6_3/mmc$ .

X-ray diffraction information gives a good picture of the electron-density distribution in the elementary cell volume. Accuracy of the image diminishes in the regions near the center of the atoms and very close to the symmetry elements

(see error distribution<sup>19-21</sup>), but for our purposes these small regions could be neglected. Corrections for the various possible deformations of x-ray-diffraction information as well as comparison with corrected values of equivalent reflections are essential to image accuracy. The corrections and comparisons we carried out are discussed in detail under Experimental Procedure.

Determination of electron densities by x-ray diffraction permits a better understanding of the interlayer forces, of the overlapping of the interlayer wave functions of the chalcogenide atoms, and of the electrical conduction in the *c* direction of the crystals. It also gives an accurate picture of the real bonds between atoms within a layer, bonds which are responsible for most of the physical properties of these crystals. Moreover, a determination of the potential distribution in the crystal is possible, permitting a calculation of band structure and electronic states.

The discrepancies between our findings and the previously proposed models lead us to hope that, as in the classical case of Si,<sup>22</sup> the electron-density determination will result in an improvement of the theoretical model.<sup>23</sup>

### EXPERIMENTAL PROCEDURE

The GaS crystals were grown by vacuum sublimation. In their axis one screw dislocation could be observed as found by Terhell and Lieth,<sup>24</sup> displaying the *AB* stacking sequence. No stacking faults were observed. The data crystal had the form of a hexagonal prism with dimensions along *a, b, c* = 0.033 × 0.039 × 0.039 cm<sup>3</sup> (volume 0.03 mm<sup>3</sup>). The crystal data for our GaS-β crystal are presented in Table I.

Details of experimental procedures are given in Table II. The sample chosen for data collection was attached with vacuum grease to the end of a thin quartz rod (diameter approximately 50 μm).

The diffraction data were treated by the STEPCAN program (Rigoult<sup>26</sup>), which is a modification of the PROFILE program for background, dead time, and Lorentz-polarization corrections. The variance of the diffracted intensities was statistically determined for three periodically measured reflections:

$$\sigma^2(F_0^2) = \sigma_{\text{count}}^2(F_0^2) + (0.01F_0^2)^2.$$

To check and increase the accuracy of absorption correction, which is of fundamental importance, 95 reflections were collected by rotation about the scattering vector. These high-order reflections ( $\theta$  between 17° and 22°) were chosen because they were unaffected by extinction, as we found from earlier MoK $\alpha$  studies. Their extinction correction was found to be about 0.96 and could be expected to be negligible for AgK $\alpha$  radiation. These observations were the basis of a least-squares fit of sample dimensions following a procedure previously described (FACIES program, Rigoult *et al.*<sup>27</sup>).

The adjusted dimensions were used for the absorption correction by numerical integration with a 12 × 12 × 10 Gaussian grid (Coppens *et al.*<sup>28</sup>). The transmission factor was found to be between 0.103 and 0.190.

In order to obtain extinction parameters unbiased by bond effects these parameters were adjusted with  $\psi$ -scan data. This procedure has been described by Rigoult, Bachet, and Becker<sup>29</sup> and was carried out by the FACIEX program. The measurements were made on 134 reflections of low order ( $\theta$  between 4° and 15°) which were found in earlier MoK $\alpha$  studies to be highly affected by extinction. The extinction proves to be anisotropic of type I with the following extinction parameters  $g_{ij}$  (× 10<sup>-4</sup>):

$g_{11}$	1.36 (9)	$g_{12}$	0.19 (5)
$g_{22}$	1.13 (5)	$g_{13}$	-0.56 (9)
$g_{33}$	1.59 (10)	$g_{23}$	-0.11 (8)

TABLE I. Crystal data for GaS-β at room temperature (293 K).

Space group:	<i>P</i> 6 <sub>3</sub> / <i>mmc</i>	
Hexagonal cell:	New values	Earlier results <sup>a</sup>
	<i>a</i> = 3.592(1) Å	3.587(3) Å
	<i>c</i> = 15.465(3) Å	15.492(7) Å
	<i>z</i> = 4	
Linear absorption coefficient:	$\mu = 87 \text{ cm}^{-1}$ (AgK $\alpha$ )	

<sup>a</sup>A. Kuhn, A. Chevy, and R. Chevalier (Ref. 25).

TABLE II. Experimental conditions for data collection (293 K).

Wavelength Ag $K\alpha_1$ : 0.5594075 Å
Apparatus: four-circle diffractometer Philips PW 1100
Monochromator: pyrolytic graphite ( $\cos^2 2\theta_M = 0.9722$ )
Scanning mode: $\theta - 2\theta$ step scan, 90 steps ( $0.02^\circ\theta$ per step), counting time: 1.33 s per step
Background determination: correlation algorithm ( $\sin\theta/\lambda$ ) <sub>max</sub> : 1.26 Å <sup>-1</sup>
Crystal size: 0.033 × 0.039 × 0.039 cm <sup>3</sup> along $a, b, c$ (volume 0.03 mm <sup>3</sup> )
Number of reflections measured: 5699
Number of symmetry-independent reflections: 615

These parameters were used to correct the extinction of all reflections by the LINEX program 74 (Becker and Coppens<sup>30</sup>).

At this stage the equivalent reflections (4–12, mean value 9) were averaged, the agreement factor  $R(F^2)$  between equivalent reflections was 3.6%, and only 14 of the 5699 reflections were eliminated because of deviation higher than  $3\sigma$  from the respective mean value. The statistical standard deviation was found to be close to the theoretical one defined above. This was an essential test of the accuracy of all data processing up to this stage, especially the correction for absorption and extinction. The number of measured reflections corresponds to 11 370 reflections in the whole reciprocal space used for later Fourier summation.

#### Structure refinement

The atomic parameters published by Kuhn *et al.*<sup>25</sup> were the starting point for full-matrix, least-squares refinements based on  $F_0^2$ , with  $\bar{\sigma}^2(F_0^2)$

as weights and scattering factors (including anomalous dispersion) for neutral Ga and S atoms from International Tables.<sup>31</sup> The results of refinements I and II are given in Table III.

There is one Ga and one S independent atom per unit cell lying in position  $\frac{1}{3}, \frac{2}{3}, z$  with site symmetry  $3m$ ; the only nonvanishing anisotropic thermal parameters  $U_{ij}$  are thus  $U_{11}, U_{22}, U_{33}$ , and  $U_{12}$  ( $U_{11} = U_{22} = 2U_{12}$ ).

We have used the program LINEX 74 (Becker and Coppens<sup>30</sup>) to refine the scale factor and the atomic parameters ( $z, U_{11}$ , and  $U_{33}$ ), see Table IV. The  $z$  parameters are of higher accuracy than in our earlier determination.<sup>25</sup>

#### Valence-charge-density determination

Our purpose was to obtain the valence charge density  $\rho_v$  within the crystal:

$$\rho_v(\vec{r}) = \rho_{\text{tot}}(\vec{r}) - \rho_{\text{core}}(\vec{r}), \quad (1)$$

where  $\rho_{\text{tot}}$  is the total electron density (for all the electrons), and  $\rho_{\text{core}}$  is the electron density for only

TABLE III. Results of refinements.

	I	II
$\sin\theta/\lambda$ range (Å <sup>-1</sup> )	0.00–1.26	0.70–1.26
Scale factor	0.998(1)	0.987(2)
$R(F)$	0.019	0.038
$R_w(F)$	0.018	0.023
$R(F^2)$	0.024	0.024
$R_w(F^2)$	0.030	0.033
$S^a$	2.59	2.29
$N_{\text{obs}}$	545	486
$N_V$	7	7

$$^a S = [\sum W(F_0^2 - F_c^2)^2 / (N_{\text{obs}} - N_V)]^{1/2}.$$

TABLE IV. Atomic parameters. Fractional coordinate  $z$  ( $\times 10^5$ ) and  $U_{ij}$  (in units of  $10^{-5}$   $\text{\AA}^2$ ).

Refinement	I	II	a
$\sin\theta/\lambda$ range ( $\text{\AA}^{-1}$ )	0.0–1.26	0.70–1.26	0.0–1.0
	Ga ( $x = \frac{1}{3}, y = \frac{2}{3}$ )		
$z$	17 082(1)	17 081(1)	17 100(10)
$U_{11}$	923(2)	895(3)	
$U_{33}$	1210(4)	1171(4)	
	S ( $x = \frac{1}{3}, y = \frac{2}{3}$ )		
$z$	60 191(2)	60 190(2)	60 160(30)
$U_{11}$	876(4)	846(5)	
$U_{33}$	1244(7)	1201(7)	

<sup>a</sup>A. Kuhn, A. Chevy, and R. Chevalier (Ref. 25).

the core electrons. The  $\rho_v$  can be computed by a Fourier summation over the reciprocal space (RR):

$$\rho_v(\vec{r}) = v_c^{-1} \sum_{\vec{H} \in \text{RR}} [F_{\text{obs}}(\vec{H})/k - F_{\text{core}}(\vec{H})] \times \exp(-2\pi i \vec{H} \cdot \vec{r}). \quad (2)$$

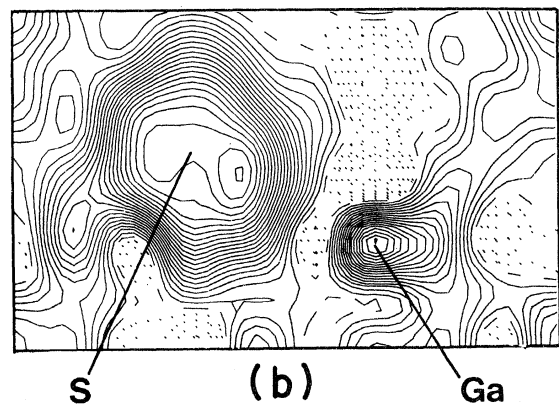
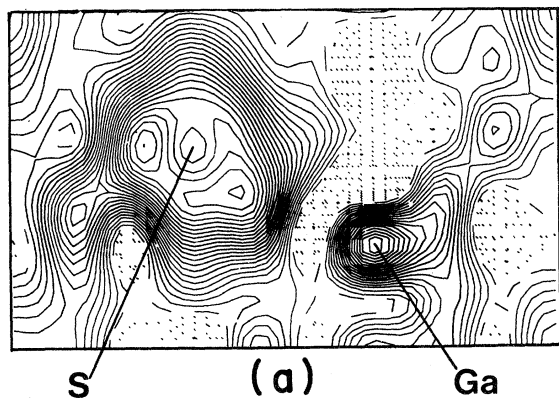


FIG. 1. GaS charge density in the (110) plane. (a) without apodization, (b) with apodization.

In this expression  $v_c$  is the cell volume,  $k$  the scale factor, and  $\vec{H}$  the diffusion vector ( $H = 2 \sin\theta/\lambda$ ).

The  $F_{\text{obs}}$  are the measured structure factors and  $F_{\text{core}}$  the theoretical structure factors corresponding to a crystal built of spherical atomic cores:

$$F_{\text{core}}(\vec{H}) = \sum_{j \in \text{cell}} f_{j,\text{core}}(\vec{H}) T_j(\vec{H}) \times \exp(2\pi i \vec{H} \cdot \vec{r}_j). \quad (3)$$

Here  $f_{j,\text{core}}$  stands for the core form factor of atom  $j$  (available from International Tables).  $\vec{r}_j$  and  $T_j$  are, respectively, the position and Debye-Waller factor of atom  $j$ .

The  $F_{\text{core}}$  were computed using the  $\vec{r}_j$  and  $T_j$  obtained from the high-order refinement II. In this case the valence contribution to structure factors is negligible so that atomic parameters obtained in this way are not biased by bonding effects.

Practically, the computation of  $\rho_v$  by Fourier summation is limited by the experimental resolution, which leads only to a partial summation up to  $H_{\text{max}}$ . To diminish the resulting diffraction or cutoff effect we used an apodization function.

We used the JIMDAP program<sup>32</sup> to calculate the electron density and the values of this density were stored on disk. They were traced by graphic processing on density maps of different planes and their numerical values printed. As is indicated by the International Tables<sup>31</sup> the form factors of the complete atom and the core are practically identical for values of  $\sin\theta/\lambda > 0.4 \text{\AA}^{-1}$ . Nevertheless, differences have been computed for  $\sin\theta/\lambda$  up to  $1.26 \text{\AA}^{-1}$ . As Hosemann and Bagchi<sup>32</sup> have shown, the contour lines of equal electron-density distribution are influenced by noise effects. They

used an apodization function to realize a smoother image, thus alternating the diffraction caused by the "cutoff" effect and the interference caused by noise.

In Fig. 1(a), we can see the (110) plane of GaS without and 1(b) with an apodization function having the following values:

$\frac{\sin\theta}{\lambda}$ ( $\text{\AA}^{-1}$ )	0-0.3	0.6	0.9
Apodization	1	0.5	0

We can see that the form of the atoms and bonds and the numerical values are practically the same, but the apodization suppresses all the structure details which result from noise effects and which have no physical meaning. The optical analogy is an attenuation of the diffraction aberration.

## RESULTS

The results<sup>40</sup> from the (110) section and the most important  $x,y,z_n$  sections for values of  $z_n$  between 0 and 0.25 and with  $\Delta z$  steps of 0.0125 are shown on density maps (Figs. 2-7). The dashed line in the

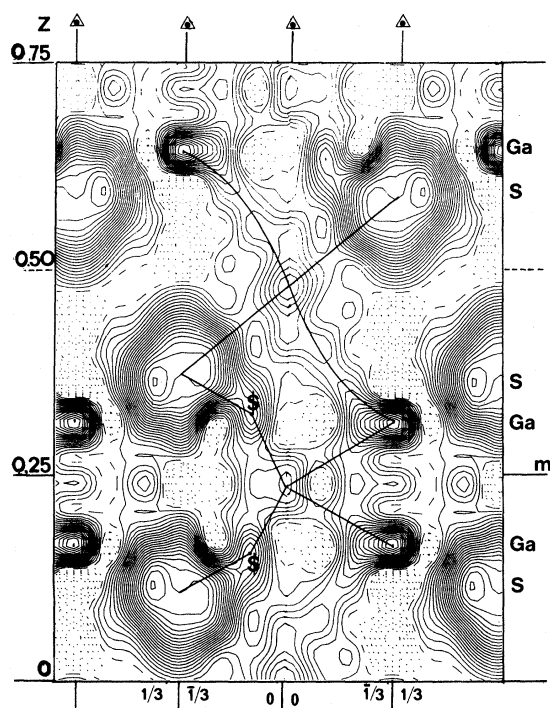
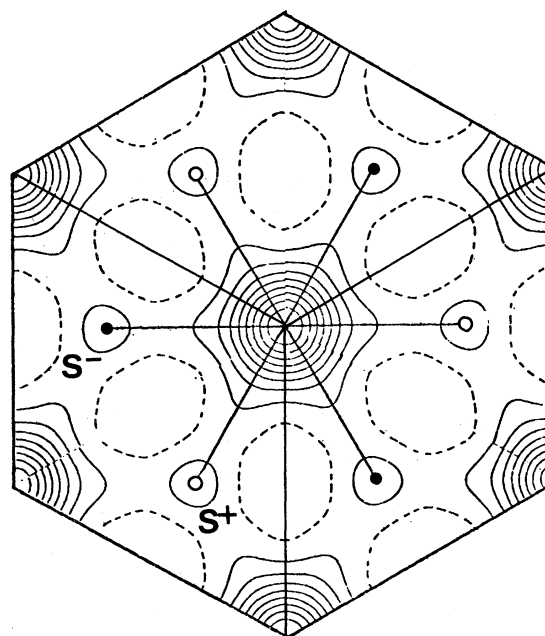


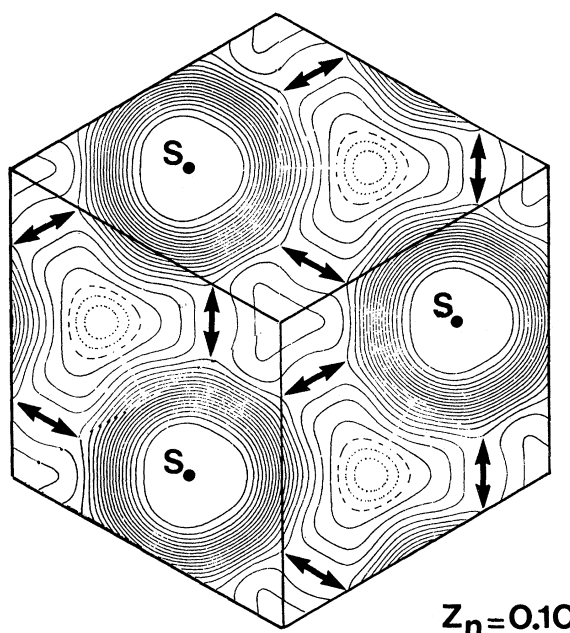
FIG. 2. GaS valence charge density in the (110) plane ( $\times$ -like inter- and intralayer bondings).



$z_n = 0.0$

FIG. 3. GaS valence charge density in the  $x,y,z_n$  plane.  $z_n=0$  (interlayer van der Waals S-S bonding).

density maps represents the zero density. The unbroken lines give increasing or decreasing charge density of  $0.05e/\text{\AA}^{-3}$ . The dotted lines indicating the "negative density" are the consequence of a "diffraction process" as in optics resulting in part



$z_n = 0.10$

FIG. 4. GaS valence charge density in the  $x,y,z_n$  plane.  $z_n=0.10$  (intralayer S-S bonding perpendicular to the  $c$  axis).

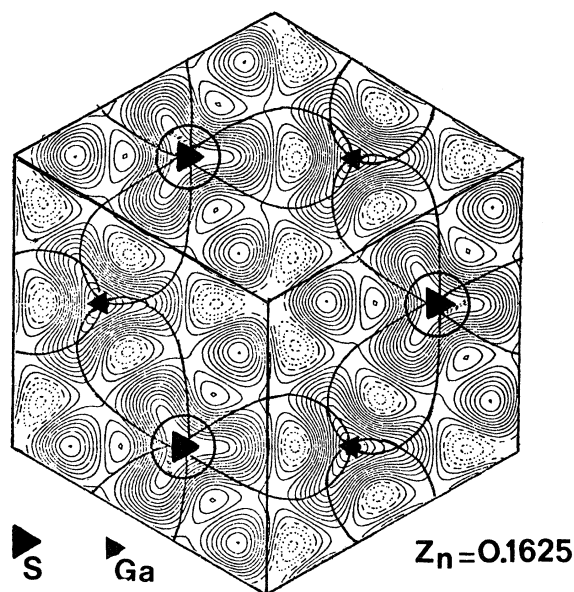


FIG. 5. GaS valence charge density in the  $x,y,z_n$  plane.  $z_n = 0.1625$  (intralayer Ga—S  $sp^3$  bonding).

from the fact that the  $\sin\theta/\lambda$  values are limited and from the existence of high-density peaks. In the volume center between four or more high-density peaks we will automatically find negative densities which have no physical sense. They are the negative parts of the Gibbs effect. They indicate the absence of an electron cloud and must be neglected. The average standard deviation of the valence density was computed to be  $0.1e/\text{\AA}^3$ .

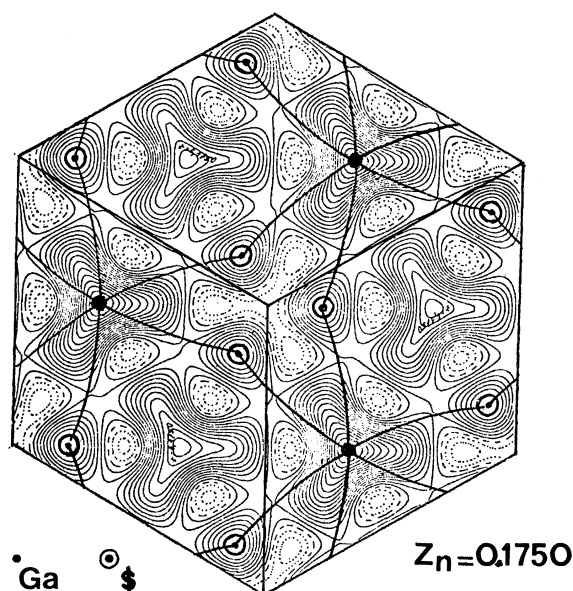


FIG. 6. GaS valence charge density in the  $x,y,z_n$  plane.  $z_n = 0.1750$  (intralayer Ga—Ga bonding perpendicular to the  $c$  axis).

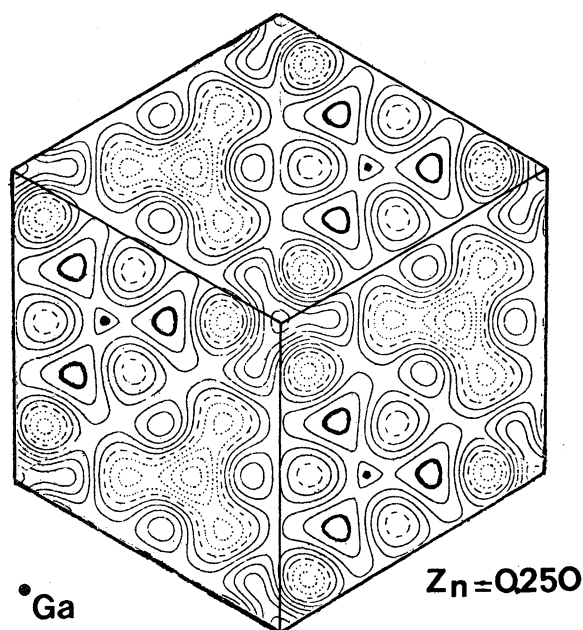


FIG. 7. GaS valence charge density in the  $x,y,z_n$  plane.  $z_n = 0.250$  (intralayer bonding of the Ga—Ga pairs in the center of the sheet).

#### Sulfur—gallium and gallium—gallium bonding

The experimental results show that the S—Ga bonding does not occur in the (110) plane as we would expect from the Ga—S total valence density of the pseudopotential model,<sup>13</sup> but the Ga—S bonding does occur around the (110) plane. The charge densities in the  $x,y,z_n$  sections ( $z_n = 0.150-0.1750$ , the Ga atom is positioned at  $\frac{1}{3}, \frac{2}{3}, 0.171$ ) show three  $sp^3$  hybrids (Fig. 5). In these sections we can also see three maxima in the  $[\bar{1}10]$  direction and the corresponding two directions by the ternary symmetry with about  $0.45e/\text{\AA}^3$  in the center of each maximum (Fig. 6). These maxima are probably the consequence of orbital overlapping of two Ga nearest neighbors in the same  $x,y,z_n$  section in such a way that each Ga atom overlaps with six nearest-neighbor Ga atoms in the same sheet. In the center of the layer, in the  $x,y,z_n$  plane with  $z_n = 0.250$ , we can observe the bonding of the two Ga atoms (one above the other) by three “bridges” (there is no direct bonding in the direction of the  $c$  axis) and the bonding of three surrounding S pairs of the layer at the origin, forming a density maximum of  $0.3e/\text{\AA}^3$  (Fig. 7).

The (110) section, Fig. 2, shows these inter- and intralayer bonds in a clear manner. We see  $\times$ -like intralayer bonds between three Ga pairs and three S pairs with a charge-density maximum  $0.3e/\text{\AA}^3$  at  $z = 0.250$  and  $0.750$  and slightly different  $\times$ -like

interlayer bonds between six Ga atoms and six S atoms around the center of symmetry at  $z=0$  and 0.50 with a density maximum of about  $0.4e/\text{\AA}^3$ .

#### Sulfur—sulfur bonding

As we can see in the (110) section (Fig. 2), the electron cloud of the four sulfur atoms in the elementary cell and of the surrounding cells spreads along the  $c$  axis with small maxima at  $z=0, 0.25, 0.50,$  and  $0.75$ . The electron cloud of one sulfur atom along the  $c$  axis has an overlapping length of  $c/4=3.866 \text{\AA}$ . We can find these maxima even in the  $x,y,z_n$  planes with  $z_n = 0$  and  $0.250$ .

In the interlayer plane  $x,y,z_n$  with  $z_n=0$ , Fig. 3, we observe an electron-density peak of about  $0.4e/\text{\AA}^3$  (eight full lines after the dashed line) on the  $a$  and  $b$  axis in the origin, surrounded by a star with six points directed toward three S atoms in the higher and three S atoms in the lower layer. Any S atom of the two layers has in this plane a density of about  $0.05e/\text{\AA}^3$ . The van der Waals forces between two consecutive layers are essentially concentrated at the origin, demonstrating that any S atom has one orbit directed toward the origin, and there are very small forces in the coordinates  $\frac{1}{3}, \frac{2}{3}, 0$  and  $\frac{2}{3}, \frac{1}{3}, 0$  the projections of the atoms.

The intralayer bonding between the S atom and its six next S neighbors is best seen in the  $x,y,z_n$  section with  $z_n=0.1$  (the position of the S atom is at  $z=0.1017$ ), Fig. 4. Between two S neighbors there are "electron bridges" with densities of about  $0.15-0.2e/\text{\AA}^3$  and density in minima between three S neighbors at the origin of  $0.05e/\text{\AA}^3$ . All S atoms overlap with six nearest-neighbors S atoms in the same sheet.

Similar density distributions can be observed in the  $x,y,z_n$  sections with values of  $z_n=0.675, 0.075,$  and  $0.0875$  and on the other side of the S atom at  $z_n=0.1125, 0.1250,$  and  $0.1375$ . In the two last sections we can see also the beginning influence of the Ga atom in the [110] direction. There is a small overlapping of the wave functions.

#### DISCUSSION

We have seen, by inspecting different sections of the crystal, that high-density regions actually bind atoms together. These high-density regions appear curved, which would seem to be in contradiction with the principle of minimization of energy. If we superpose different sections or if we build up a three-dimensional model we can arrive at a more

precise observation. It becomes apparent that these curved bonds share long common parts and overlap (for example at the point  $\$$  in Figs. 2 and 6), a situation which "minimizes" the total bond length of the crystal. This provides an explanation for the fact that high-density regions are not straight or even localizable in only one plane and that they fill atomless interlayer or intralayer regions.

In a similar way  $\times$ -like bonds between four coplanar atoms are shorter than the correspondent quadrilateral bonds. In phonon studies, this type of bonding has qualitative consequences and prior to our experiments, Polian *et al.*<sup>33</sup> has already introduced a fifth force between Ga and S of adjacent half-layer to fit experimental dispersion curves with those calculated, using a rigid-ion model with axially symmetric forces. They even suggested an additional interaction between the center of the Ga—Ga bonds. The  $\times$ -like intralayer bonding we found (Fig. 2) seems to agree with their interpretation of the phonon-dispersion curve.

At very high pressure Polian *et al.*<sup>34</sup> have seen that intralayer and interlayer bondings tend towards the same value. Our measurements, at normal pressure, do show a similarity in their  $\times$ -like shape. The former bondings are stronger than the latter and it can be presumed that they become equal at very high pressures. Later work will verify whether these two instances of overlapping and types of Ga—S bonding are responsible for the  $\beta$  type.

An initial, simplified calculation shows a charge of about 5.5 electrons around the S cores and of only 0.2 electron around the Ga cores as in the case of a metal. In GaS, the Ga-Ga distance is  $2.449 \text{\AA}$ , whereas the shortest distance between two Ga atoms in metallic  $\alpha$ -phase gallium is  $2.437 \text{\AA}$  (Bradley<sup>35</sup>). The  $\alpha$  phase is the only stable phase of metallic gallium. In the metastable phases  $\beta$  (Ref. 36),  $\gamma$  (Ref. 37), and  $\delta$  (Ref. 38), the Ga-Ga distance is greater than  $2.60 \text{\AA}$ . This confirms the metallic nature of the intralayer Ga—Ga bond in GaS.

We are now calculating the electronic structure of GaS with a self-consistent local-density formalism which differs from that used by Zunger and Freeman.<sup>38</sup> Initial results for total valence-electron density seem to be in very good agreement with our experimental results. Later, we would like to study the electron density due to each state (band) separately, which will enable us to determine the contribution of each valence band to the chemical bonds in GaS.

## CONCLUSION

Our experimental results show the presence not only of bonding between Ga-S and Ga-Ga nearest neighbors in the elementary cell as predicted by the pseudopotential model but also of bonding between Ga and S next-nearest neighbors in the same elementary cell and with atoms in the surrounding elementary cells. The latter bonds cannot be predicted by the model used in the pseudopotential

method.

This unusual electron density may arise from the fact that, in GaS, atoms are not closely packed. This arises from the noncomplementarity of the valence (groups III and VI) of the components. The  $d$  inner state of Ga has probably some influence on this crystalline structure.

We would hope that the real bonding found experimentally will stimulate a rethinking and reshaping of the theoretical model.

\*Equipe de Recherche associée au CNRS.

†Laboratoire associé au CNRS.

- <sup>1</sup>A. Polian, K. Kunc, and A. Kuhn, in *Physics of Semiconductors, Proceedings of the 13th International Conference, Rome, 1976*, edited by F. G. Fumi (Typographia Marves, Rome, 1976), pp. 392–395.
- <sup>2</sup>A. Kuhn, A. Chevy, and A. Chevalier, *Phys. Status Solidi A* **31**, 469 (1975).
- <sup>3</sup>R. Le Toullec, M. Balkanski, J. M. Besson, and A. Kuhn, *Phys. Lett.* **55A**, 245 (1975).
- <sup>4</sup>G. Ottaviani, C. Canali, F. Nava, Ph. Schmid, E. Mooser, R. Minder, and I. Zschokke, *Solid State Commun.* **14**, 933 (1974).
- <sup>5</sup>F. Bassani and G. Pastori, *Nuovo Cimento* **50**, 95 (1967).
- <sup>6</sup>H. Kamimura and N. Nakao, *J. Phys. Soc. Jpn.* **24**, 1313 (1968).
- <sup>7</sup>J. V. McCanny and R. B. Murray, *J. Phys. C* **10**, 1211 (1977).
- <sup>8</sup>J. Robertson, *J. Phys. C* **12**, 4777 (1979).
- <sup>9</sup>A. Bourdon, Thesis, Paris, 1971 (unpublished); A. Bourdon, *J. Phys. (Paris) Colloq.* **35**, 261 (1974).
- <sup>10</sup>M. Schlüter, *Nuovo Cimento* **33**, 313 (1972).
- <sup>11</sup>E. Mooser, I. Ch. Schlüter, and M. Schlüter, *J. Phys. Chem. Solids* **35**, 1269 (1974).
- <sup>12</sup>M. Schlüter and M. L. Cohen, *Phys. Rev. B* **14**, 424 (1976).
- <sup>13</sup>M. Schlüter, J. Camassel, S. Kohn, J. P. Vojtchovsky, Y. R. Shen, and M. L. Cohen, *Phys. Rev. B* **13**, 3534 (1976).
- <sup>14</sup>Y. Depeursigne, *Nuovo Cimento* **38 B**, 153 (1977).
- <sup>15</sup>Y. Depeursigne, E. Doni, R. Girlanda, A. Baldereschi, and A. Maschke, *Solid State Commun.* **27**, 1949 (1971).
- <sup>16</sup>G. Margaritondo, J. E. Rowe, and S. B. Christman, *Phys. Rev. B* **15**, 3844 (1977).
- <sup>17</sup>J. M. Thomas, I. Adams, R. H. Williams, and M. Barbu, *J. Chem. Soc. Faraday Trans. II* **68**, 755 (1972).
- <sup>18</sup>R. H. Williams, J. V. McCanny, R. B. Murray, L. Levy, and P. C. Kerneny, *J. Phys. C* **10**, 1223 (1977).
- <sup>19</sup>E. D. Stevens, J. Rys, and P. Coppens, *J. Am. Chem. Soc.* **99**, 265 (1977).
- <sup>20</sup>E. D. Stevens and P. Coppens, *Acta Crystallogr. Sec. A* **32**, 915 (1976).
- <sup>21</sup>B. Rees, *Acta Crystallogr. Sec. A* **34**, 254 (1978).
- <sup>22</sup>Y. W. Yang, P. Coppens, *Solid State Commun.* **15**, 1555 (1974).
- <sup>23</sup>J. R. Chelikowsky and M. L. Cohen, *Phys. Rev. B* **10**, 5095 (1974).
- <sup>24</sup>J. C. J. M. Terhell and R. M. A. Lieth, *J. Cryst. Growth* **13-14**, 380 (1972).
- <sup>25</sup>A. Kuhn, A. Chevy, and R. Chevalier, *Acta Crystallogr. Sec. B* **32**, 983 (1976).
- <sup>26</sup>J. Rigoult, *J. Appl. Cryst.* **12**, 116 (1979).
- <sup>27</sup>J. Rigoult, A. Tomas, and C. Guidi-Morosini, *Acta Crystallogr. Sec. A* **35**, 587 (1979).
- <sup>28</sup>P. Coppens, L. Leiserowitz, and D. Rabinovitch, *Acta Crystallogr.* **18**, 1035 (1965).
- <sup>29</sup>J. Rigoult, B. Bachet, and P. J. Becker, *Acta Crystallogr.* (in press).
- <sup>30</sup>P. J. Becker, and P. Coppens, *Acta Crystallogr. Sec. A* **31**, 417 (1975).
- <sup>31</sup>*International Tables for X-ray Crystallography*, (Kynoch, Brimingham, 1974), Vol. IV.
- <sup>32</sup>R. Hosemann and S. N. Bagchi, *Nature* **171**, 785 (1953).
- <sup>33</sup>A. Polian, K. Kunc, R. Le Toullec, and B. Dorner, in *Proceedings of the Conference on Physics of Semiconductors, Edinburgh, 1978*, edited by B. L. H. Wilson (Institute of Physics, Bristol, 1979), p. 907.
- <sup>34</sup>A. Polian, J. C. Chervin, and J. M. Besson, *Phys. Rev. B* **22**, 3049 (1980).
- <sup>35</sup>A. J. Bradley, *Z. Kristallogr. A* **91**, 302 (1935).
- <sup>36</sup>L. Bosio and A. Defrain, *Acta. Crystallogr. Sec. B* **25**, 995 (1969).
- <sup>37</sup>L. Bosio, H. Curien, M. Dupont, and A. Rimsky, *Acta Crystallogr. Sec. B* **28**, 1974 (1972).
- <sup>38</sup>L. Bosio, H. Curien, M. Dupont, and A. Rimsky, *Acta Crystallogr. Sec. B* **29**, 367 (1973).
- <sup>39</sup>A. Zunger, and A. J. Freeman, *Phys. Rev. B* **15**, 4716 (1977).
- <sup>40</sup>See AIP document no. PAPS 25-4081-7 for 7 pages of a list of the form factors and the  $X, Y, Z_n$  sections for  $Z_n = 0 - 0.2625$  in steps of  $\Delta Z_n = 0.0125$ . Order by PAPS number and journal reference from American Institute of Physics, Physics Auxiliary Publication Service, 335 East 45th Street, New York, N.Y. 10017. The price is \$1.50 for a microfiche, or \$5.00 for a photocopy. Airmail additional. Make checks payable to the American Institute of Physics.